
Predication of Forming Limit Diagram and Spring-back during SPIF process of AA1050 and DC04 Sheet Metals

Marwan T. Mezher[†], Osamah Sabah Barrak[‡], Sami Ali Nama^{††}, Rusul Ahmed Shakir[†]

[†] Middle Technical University, Institute of Applied Arts, Baghdad, Iraq

[‡] Middle Technical University, Institute of Technology - Baghdad, Iraq

^{††} Middle Technical University, Engineering Technical College – Baghdad, Iraq

*Corresponding Author E-mail: marwantahir90@gmail.com

ABSTRACT: Incremental sheet forming process (ISF) has been demonstrated its large potential to manufacture and fabricate three-dimensional complex shapes which are needed in different industrial sectors. In this paper, an attempt has been made in term of formability to identify the maximum forming angle of AA1050 aluminium alloy and DC04 carbon steel through manufacturing a frustum cone by using single point incremental forming process (SPIF). Investigation of forming angle is considered as an important index for choosing the optimal and suitable forming process parameters to avoid the demerits of crack initiation and fracture risks. In order to make a satisfying investigation, a numerical simulation is developed at the same of the experimental parameters, therefore, ANSYS V.18 (workbench LS-DYNA) was applied to create A 3D- finite element model of frustum cone product with different forming angle and the analysis of the results has been done with aid of LS-PREPOST software to evaluate the influence of forming angle on the forming limit diagram (FLD), residual stresses, and spring-back. The Cowper Symonds power law hardening was adopted to simulate the elastic-plastic behavior and assuming the isotropic properties were used to model the plasticity behavior of AA1050 aluminum alloy and DC04 carbon steel during the SPIF process. The results exhibit that the DC04 carbon steel has the highest formability where the maximum forming angle reaches 75° whereas it was 72° for AA1050 aluminum alloy.

KEYWORDS: SPIF, Forming angle, FEM, FLD, Spring-back, Residual Stress.

INTRODUCTION

Nowadays, single point incremental forming process (SPIF) has become more promising and prominent to achieve the current requirements and trends in the industry due to its merits in comparison with the conventional forming process [1, 2]. These benefits of the incremental sheet forming process (ISF) involved the enhancement in the formability of sheet metal products [3, 4] and fulfilled the requirements of different industrial sectors such as aerospace, biomedical applications and the automobile industry [5-7]. Numerous studies have attempted to elucidate the relationship between the SPIF process parameters and the maximum formability of various products shape. Kumar A, et al. [8] made an experimental study of AA2024 during SPIF process of the influence the wall angle, tool diameter, sheet thickness on the forming force, they found that the axial peak force increase with the increase in forming an angle, tool diameter and sheet thickness. Honarpisheh M, et al. [9] studied the formability by means of experimental and numerical investigation during the electric hot-assisted SPIF process, the results indicate that the formability was reduced with an increase in step size and tool diameter.

Liu Z, et al. [10] concluded that the forming force increased with the rise in the forming angle of the product. Dufloy JR, et al. [11] analyzed the impact of local heating by using the laser-assisted SPIF process on the formability of 65Cr2 sheet product. Results indicated that the forming angle reaches 64° by using a laser-assisted SPIF process, while it was 57° when the SPIF process performed at room temperature. Kumar A and Gulati V [12] noticed a distinct increase in the axial peak force with the rise of the wall angle. Golabi S and Khazaali H [13] found that the formability of SS304 has an opposite relationship with step size and feed rate. Filce L, et al. [14] conducted a series of experiments on AA1050-O and findings exhibit that the tangential peak force raised as a result of the wall angle increased. Mezher M.T, et.al [15, 16] investigated experimentally and numerically the impact of Nano particles additive on the quality of formed products through using different forming processes and the results showed a significant improvement in the accuracy of the formed parts due to using Nano powder.

Lehtinen P, et al. [17] made a comparative analysis of the formability in terms of maximum forming angle manufactured at room temperature and high temperatures using laser irradiation as a heating media for copper and aluminum during the SPIF process.

Two papers tested the effect of feed rate on the formability of components during the SPIF process and showed that it increases owing to an increase in feed rate [18, 19]. While in the contrast other papers reveal the opposite findings where the reduce the feed rate leads to rise in the formability of products [20-22]. Two papers [23, 24] analyzed the impact of spindle speed on the formability of various sheet materials and the results indicate that the formability increase as a result of increasing spindle speed. Namer N. S, et.al [25] investigated the influence of lubricant viscosity on the parameters of the SPIF process of polymer sheets and findings pointed out a significant improvement in these parameters as a consequence of increasing the lubricant viscosity. Literature shows that the maximum formability created during SPIF is of great concern because it is identified the maximum limit of formed sheet material. Consequently, it is important to investigate the formability of components to prevent the occurrence of drawbacks and fractures in the final product. Therefore, the present work intends to determine the maximum formability in term of forming angle of AA1050 aluminum alloy and DC04 carbon steel for conical frustum have been fabricated during SPIF process by means of experimental and numerical investigation in order to evaluate the effect of different forming angle on the forming limit diagram (FLD) and spring-back phenomenon. In order to reduce the friction environment between the forming tool and sheet surfaces, hybrid Nano lubricant additives have been used depending on the findings observed by Namer NSM, et.al, [26].

EXPERIMENTAL SETUP

Single point Incremental forming (SPIF)

The experimental work is conducted on a TX32 CNC milling machine and the fixture which is utilized to mount the sheet metal was fixed on the table of the CNC milling machine. Since this operation was controlled by the CNC machine, therefore no special die is required as in conventional sheet metal forming operations and the absence of die leads to decrease in the cost of forming requirements. SPIF is a process where the blank sheet gets deformed to produce the final shape by continuous application of small incremental deformations. A spherical shaped forming tool with a diameter of 16 mm which is attached in the vertical part of the CNC milling machine and follow the tool path which was selected as a spiral to get a conical product with a step size equal to 0.05 mm per revolution, spindle speed 450 rev/min, and feed rate 600 mm/min were used as working conditions. The fixture is fabricated to performed the SPIF experiments and it is composed of the clamping plate, backing plate, upper and lower plate as well as the support pillar and all fixture tools are fixed on the CNC milling machine as illustrated in figure 1. Square sheets of AA1050 aluminum alloy and DC04 carbon steel with (200 X 200 X 1) mm were used in the current paper.



Figure 1. Fixture tools on CNC milling machine

Material Properties

AA1050 aluminium alloy and DC04 carbon steel with 1 mm thickness have been used in the present investigation. A group of tensile experiment was performed to characterize the mechanical properties with aid of double hydraulic acting press with 30 ton as a maximum capacity according to both sheet metals depend on to ASTM-E8 standard [27], the mechanical properties are presented in table 1.

Table 1. Mechanical properties of and AA1050 aluminum alloy and DC04 carbon steel

Material Property	AA1050	DC04
Yield Strength (MPa)	33	215
Tensile Strength (MPa)	152	335
Strength coefficient (K) (MPa)	218	510
Hardening exponent (n)	0.23	0.21
Poisson's ratio	0.33	0.3
Young modulus (GPa)	69	210

FINITE ELEMENT MODEL

In order to evaluate the formability of the truncated cone of AA1050 aluminium alloy and DC04 carbon steel during the SPIF process, a numerical model of SPIF is compulsory to fulfil the analysis of the accuracy of the formed product. The purpose of the finite element model is to calculate the stress, strain, , forming limit curve (FLC), and spring-back along the wall of formed parts and compare these results with experimental findings for verification. An explicit dynamic simulation is conducted using ANSYS V.18 (LS- DYNA model) to create the model whereas the analysis of the results had been done through using LS-PREPOST software. Owing to the lack of the tool path, a full model of the SPIF process was constructed. The sheet metal behaviour was assumed an elastic–plastic, the elastic properties were assumed based on Young modulus and Poisson's ratio such as described in table 1. the Cowper Symonds power-law hardening model is adopted to simulate the plasticity behaviour of blank sheet. The sheet metal is meshed using fully integrated shell element formulation with 7 points integration through-thickness and the element size was 0.002 mm. the spherical forming tool, backing plate, and clamping were modelled to be rigid bodies while the blank sheet was assumed as a deformable body. The contact interface between the parts (forming tool – blank sheet, clamping plate – blank sheet and blank sheet – backing plate) are modelled based on the surface to surface forming formulation and soft constraint formulation is selected as a penalty, and Coulomb's friction law was used to describe and solve the frictional interface impact between the contact interface parts, moreover, the coefficient of friction was chosen to equal 0.0311 for hybrid Nano powder (MoS₂ and CuO) which were mixed with sunflower oil as it is observed by Namer NSM, et.al, [26] .

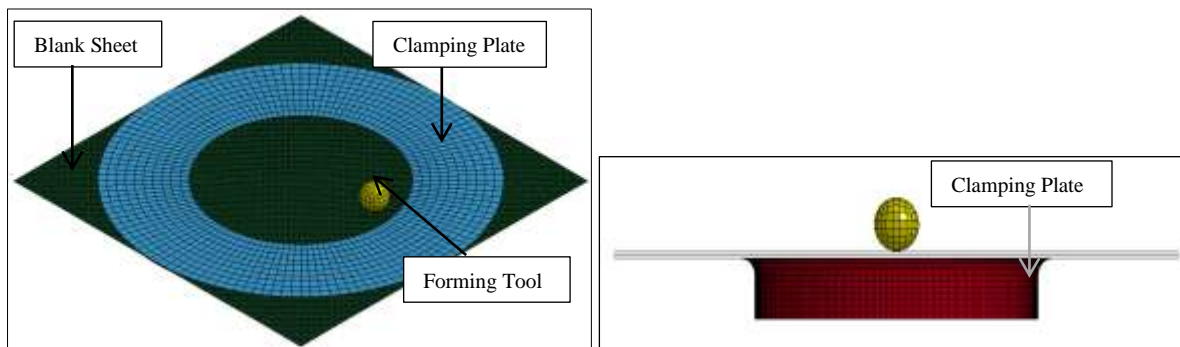


Figure 2. FE meshed model of SPIF process

RESULTS AND DISCUSSIONS

Formability

In the SPIF process, the resultant formability is much higher than in traditional metal forming process such as stamping and deep drawing processes, in the present study the maximum wall angle shall be considered as an indicator to the formability where the specimens of AA1050 aluminium alloy and DC04 carbon steel with 1 mm thickness have been formed in the range of wall angles such as 45°, 55°, 65°, 70 and 75° to determine the safe formability limit of forming angle for each sheet metals used in the current work and after the completion of each experiment during SPIF process and made observations on the final product with each angle to identify if there is any indication of fracture appears or not. The results of the experimental and FEM results refer to that the DC04 carbon steel gives the higher forming angle reaches up to 75° without ant observation of failure or occurrence of cracks while the AA1050 give the lower forming angle extends up to 72°, as illustrated from figures 3 and 4.

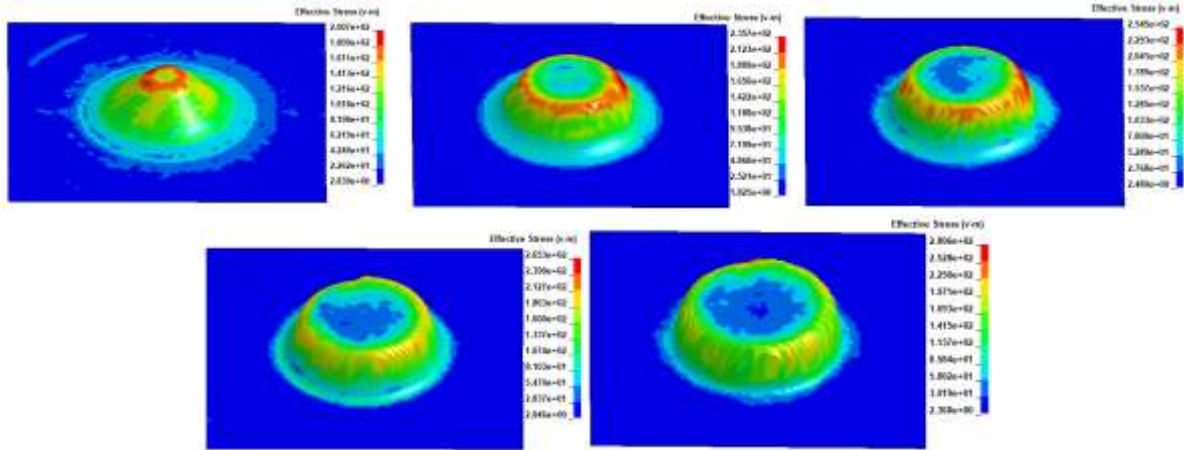


Figure 3. FEM results of wall angle of AA1050

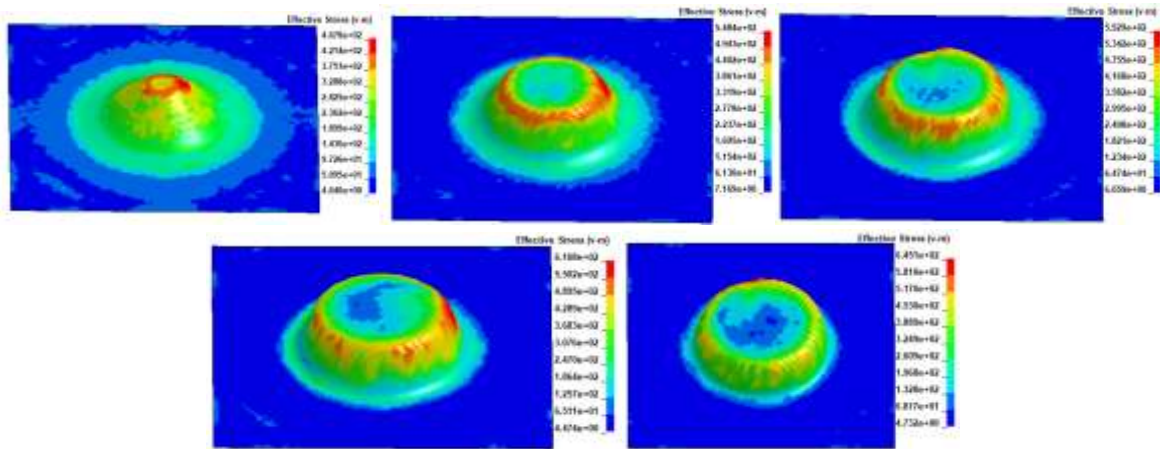


Figure 4. FEM results of wall angle of DC04

Figure 5 depicts the correlation between the Von-Mises stress and forming an angle of both AA1050 aluminium alloy and DC04 carbon steel, and as it was apparent from figure 5, there is a notable increase in Von-Mises stresses as a consequence of increasing the wall angle due to the fact that more material available for local deformation under the forming tool for each pass, consequently more forming force required to form the blank sheet and that causing an increase in Von-mises stresses. furthermore, the elements nearby the bottom of the cone product suffered from high stress in comparison with those elements on the wall product or the part of the product which is in direct contact clamping plate. Another interesting observation is that Von-Mises stresses generated in the formed parts of AA1050 is lower than of these stresses of DC04 carbon steel owing to the low tensile strength of AA1050 in compared to DC04 as it is clearly shown in table 1.

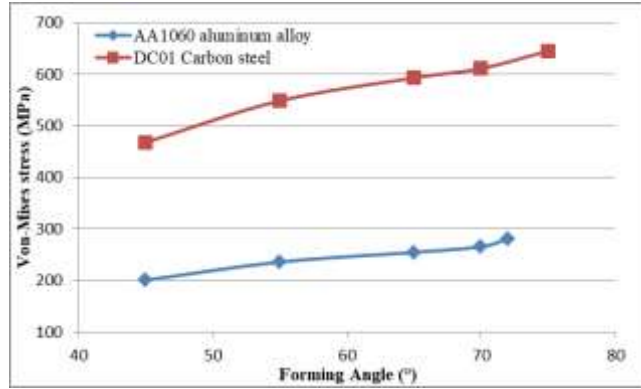


Figure 5. Correlation between Von-Mises stress and forming angle

Forming limit diagram (FLD)

Forming of sheet materials as it well known is identified through localized necking and fracture in various sheet metal forming processes. Therefore, the forming limit diagram which is deemed an admissible common practice to characterize and appreciate the forming limits in industrial sectors. In order to understand the effect of forming angle on the FLD trend of AA1050 aluminium alloy and DC04 carbon steel during the SPIF process, the mechanical grid patterns were printed on the surface of sheet metal specimens as depicted in figure 6, FLD constricts of the true minor and major strains that are plotted in X and Y-axis respectively as shown in figure 7. Consequently, after the completion of the SPIF process, these grid patterns were deformed and became elliptical shape with major and minor diameters in the X and Y-axis. Measurements of those diameters which represent the major and minor strains in FLD curves were achieved depend on image analysis with the assist of AutoCAD software. Figures 8 and 9 present the FEM and experimental results of FLD of AA1050 aluminium alloy and DC04 carbon steel respectively.



Figure 6. Specimens of formed parts

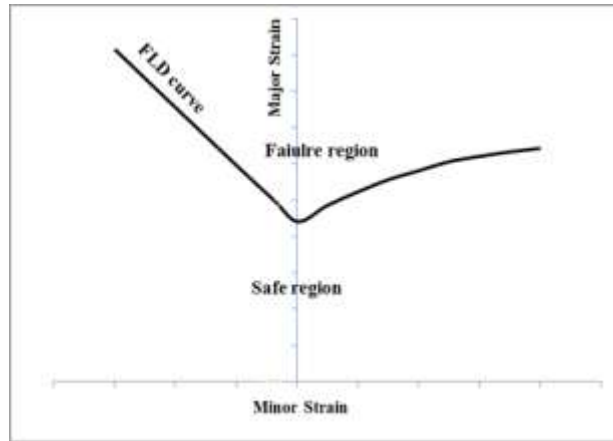


Figure 7. Schematic diagram of forming limit diagram (FLD) [16].

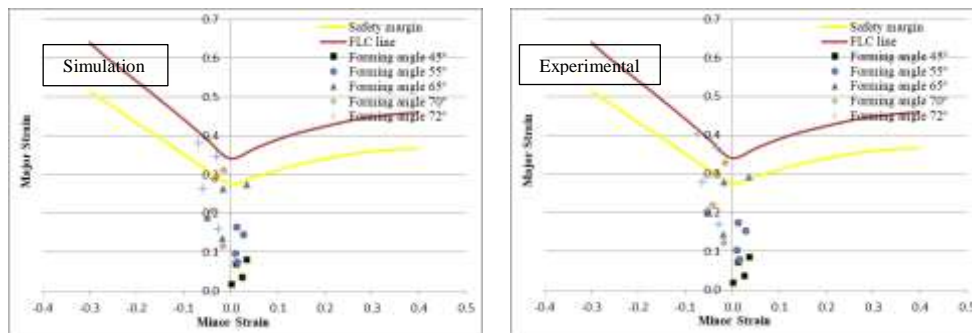


Figure 8. FLD of AA1050 with the varying of forming angle

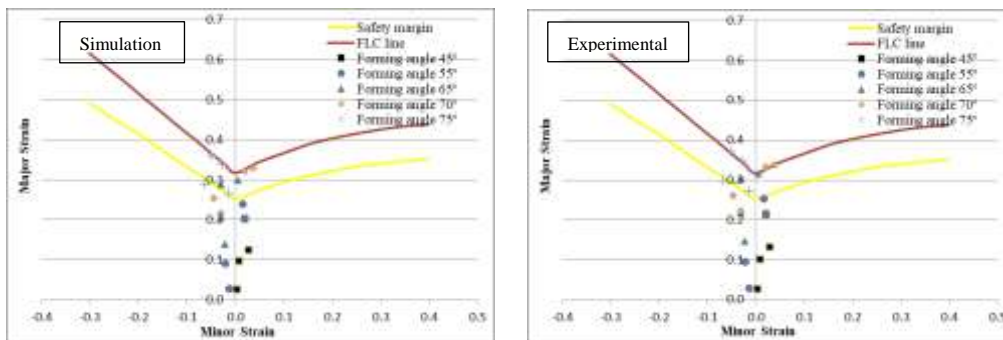


Figure 9. FLD of DC04 with the varying of forming angle

It worth noticing from the above figures, the FLD curves in terms of minor and major strains of angles under 55° reveal the safe points and there is no indication of the possibility of initiation of cracks and later occurrence of failure due generated very little deformation. This is because the sheet blanks which are formed with these specified angles does not suffer from the more stretching operation which was high for angles larger than 65° and the minor and major strains were higher than those of angles less than 55° , therefore when the stretching increase that results from more deformation for the same pass during SPIF process and this pass deformed nearly twice times at angle 65° than 45° . The predicted FLD from the FEM simulation corresponded fairly with the experimental data. Another interesting observation had been noted from previous figures, the FLD curves present two fashion, firstly there are some point laying on the positive part of the curve which is indicated to that, these points are suffered from stretch deformation and formed with biaxial strain condition that is applied from forming tool. Secondly, the other points took place on the negative part of the curve owing to that the state of deformation is altered from biaxial to uniaxial and hence the sheet blanks deformed with stretch operation at the initial increments of process and then subjected to components of deformation constructed from radial and stretching deformation. As it was obvious from the figures there are some points of strain relying between the safety margin

(yellow line) and fracture forming curve (red line) which means these points are safe but it still critical due to nearby them to the critical curve (red line).

Spring-back analysis

Spring-back phenomenon is vital concern in the ISF process and a precise calculation, and prediction of spring-back is fundamental because it has a major influence on the quality of final product during SPIF process. In the present study, the spring-back is analysed through the angle difference before and after released the samples of the truncated cone from the fixture tools due to produce the residual stress in the frustum cone as well as the elastic recovery which is results in a dimensional change at the forming angle of formed components. Experimental calculation of the spring-back angle was achieved by cutting the samples into half sections and measure the deviation between designed and resultant angle with the assist of image analysis by using AutoCAD program and later the final spring-back is determined based on the following formula:

$$\text{Spring-back angle} = (\text{design forming angle of the truncate cone} - \text{measured forming angle} / \text{design forming angle of the truncate cone}) * 100\%.$$

The benefit of using workbench LS-DYNA model in this paper to analyze the spring-back because the LS-PREPOST which is used to analysis the response of the process parameters on the results, give the value of spring-back angle directly after removing the fixtures tool. Figure 10 portrays the FEM simulation and experimental variation in spring-back with respect to the forming angle of AA1050 aluminum alloy and DC04 carbon steel respectively. As it can be seen, the spring-back has A direct relationship with the forming angle and it increases with rise the wall angle. The possible reason for that, when the sheet metal formed with high forming angle that is contributed to generate more residual stresses in formed cone after the completion of the SPIF process as it obvious from figure 4. Another observation had been noticed the formed parts of DC04 carbon steel show slightly higher spring-back value in comparison with AA1050 aluminum alloy at the same forming angles as a consequence of more residual stresses had been generated in the formed components of DC04 carbon steel. Numerical findings of spring-back show good agreement with the experimental results.

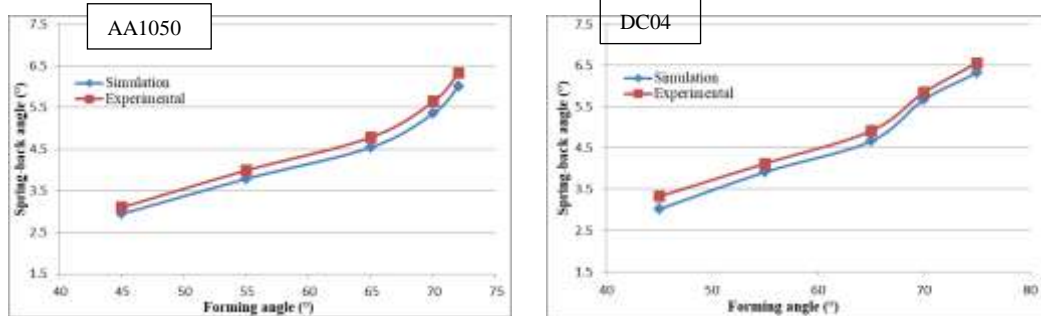


Figure 10. Variation in spring-back angle with different forming angle

CONCLUSIONS

In this study, the experimental and numerical investigation of the SPIF process of AA1050 and DC04 sheet metals was carried out. The results of the study can be drawn as follows:

1. The highest value of forming angle was achieved of a truncated cone is 75° for DC04 and 72° for AA1050.
2. Von-Mises stress has a direct relationship with the forming angle.
3. Forming limit diagram (FLD) show extremely effected with rising of forming angle and the critical major and minor strains were generated with higher wall angles.
4. The degree of spring-back is increased as a result of increasing the wall angle.
5. DC04 carbon steel at different wall angle exhibits roughly good results in comparison with AA1050 aluminium alloy.
6. Cowper Symonds power-law hardening model is good to build the FEM model of SPIF process and the numerical results match fairly with the experimental data.

REFERENCES

- [1] S. Gatea, H. Ou, and G. McCartney, "Review on the influence of process parameters in incremental sheet forming", *Int. J. Adv. Manuf. Techn.*, Vol. 87, No. 1–4, Pp. 479–499, 2016. doi: 10.1007/s00170-016-8426-6.
- [2] T. McAnulty, J. Jeswiet, and M. Doolan, "Formability in single point incremental forming: a comparative analysis of the state of the art", *CIRP J. Manuf. Sci. Techn.*, 2016. doi: <http://dx.doi.org/10.1016/j.cirpj.2016.07.003> 1755-5817/.
- [3] K. Roll, "Simulation of sheet metal forming – Necessary developments in the future", Keynote paper NUMISHEET, 2008.
- [4] O.S. Barrak, M.L. Saad, M.T. Mezher, S.K. Hussein, and M.M. Hamzah, "Joining of Double Pre-Holed Aluminum Alloy AA6061-T6 to Polyamide PA using Hot Press Technique", In *IOP Conference Series: Materials Science and Engineering*, Vol. 881, No. 1, Pp. 012062, 2020.
- [5] R. Katipelli, A. Agarwal, and N.B. Dahotre, "Laser surface engineered TiC coating on 6061 Al alloy: microstructure and wear", *Appl. Surf. Sci.*, Vol. 153, Pp. 65–78, 2000.
- [6] Y.H. Ji and J.J. Park, "Incremental forming of free surface with magnesium alloy AZ31 sheet at warm temperatures", *Transactions of Nonferrous Metals Society of China*, Vol. 18, Pp. s165–s169, 2008.
- [7] V. Oleksik, A. Pascu, C. Deac, R. Fleacă, O. Bologa and G. Racz, "Experimental study on the surface quality of the medical implants obtained by single point incremental forming", *Int. J. Mater. Form.*, Vol. 3 Suppl 1, Pp. 935–938, 2010. doi: 10.1007/s12289-010-0922-x.
- [8] A. Kumar, V. Gulati, and P. Kumar, "Investigation of process variables on forming forces in incremental sheet forming", *Int. J. Eng. Technol.*, Vol. 10, Pp. 680–684, 2018.
- [9] M. Honarpisheh, M.J. Abdolhoseini, and S. Amini, "Experimental and numerical investigation of the hot incremental forming of Ti–6Al–4V sheet using electrical current", *Int. J. Adv. Manuf. Technol.*, Vol. 83, No. 9–12, Pp. 2027–2037, 2016.
- [10] Z. Liu, Y. Li, and P.A. Meehan, "Experimental investigation of mechanical properties, formability and force measurement for AA7075-O aluminum alloy sheets formed by incremental forming", *Int. J. Precis. Eng. Manuf.*, Vol. 14, No. 11, Pp. 1891–1899, 2013.
- [11] J.R. Dufloy, B. Callebaut, J. Verbert, and H. De Baerdemaeker, "Improved SPIF performance through dynamic local heating", *Int. J. Mach. Tools Manuf.*, Vol. 48, No. 5, Pp. 543–549, 2008.
- [12] A. Kumar, and V. Gulati, "Experimental investigations and optimization of forming force in incremental sheet forming", *Sādhanā*, Vol. 43, No. 10, Pp. 159, 2018.
- [13] S. Golabi, and H. Khazaali, "Determining frustum depth of 304stainless steel plates with various diameters and thicknesses by incremental forming", *J. Mech. Sci. Technol.*, Vol. 28, No. 8, Pp. 3273–328, 2014.
- [14] L. Filice, G. Ambrogio, and F. Micari, "On-line control of single point incremental forming operations through punch force monitoring", *CIRP Ann. Manuf. Technol.*, Vol. 55, No. 1, Pp. 245–248, 2006.
- [15] M.T. Mezher, N.S. Namer, and S.A. Nama, "Numerical and Experimental Investigation of Using Lubricant with Nano Powder Additives in SPIF Process", *International Journal of Mechanical Engineering and Technology*, 9 (13), Pp. 968-977, 2018.
- [16] M.T. Mezher, M.L. Saad, O.S. Barrak and R.A. Shakir, "Finite Element Simulation and Experimental Analysis of Nano Powder Additives Effect in the Deep Drawing Process", *International Journal of Mechanical & Mechatronics Engineering IJMME-IJENS*, 20(01), 166-180, 2020.
- [17] P. Lehtinen, T. Väisänen, M. Salmi, "The effect of local heating by laser irradiation for aluminum, deep drawing steel and copper sheets in incremental sheet forming", *Phys Procedia*, Vol. 78, Pp. 312–319, 2015.
- [18] L. Bagudanch, M.L. Garcia-Romeu, G. Centeno, A. Elas-Ziga, and J. Ciurana, "Forming Force and Temperature Effects on Single Point Incremental Forming of Polyvinylchloride", *Journal of Materials Processing Technology*, 219, Pp. 221– 229, 2015. <http://dx.doi.org/10.1016/j.jmatprotec.2014.12.004>.

- [19] G. Ambrogio, and F. Gagliardi, “Temperature Variation During High-Speed Incremental Forming on Different Lightweight Alloys”, *International Journal of Advanced Manufacturing Technology*, Vol. 76, No. 9–12, Pp. 1819–1825, 2015. <http://dx.doi.org/10.1007/s00170-014-6398-y>.
- [20] M. Ham, and J. Jeswiet, “Single Point Incremental Forming and the Forming Criteria for AA3003”, *CIRP Annals – Manufacturing Technology*, Pp. 55, No. 1, Pp. 241–244, 2006. [http://dx.doi.org/10.1016/S0007-8506\(07\)60407-7](http://dx.doi.org/10.1016/S0007-8506(07)60407-7).
- [21] V.S. Le, A. Ghiotti, and G. Lucchetta, “Preliminary Studies on Single Point Incremental Forming for Thermoplastic Materials”, *International Journal of Material Forming*, Vol. 1, No. 1, Pp. 1179–1182, 2008. <http://dx.doi.org/10.1007/s12289-008-0191-0>.
- [22] G. Hussain, L. Gao, and Z.Y. Zhang, “Formability Evaluation of a Pure Titanium Sheet in the Cold Incremental Forming Process”, *International Journal of Advanced Manufacturing Technology*, Vol. 37, No. 9–10, Pp. 920–926, 2008. <http://dx.doi.org/10.1007/s00170-007-1043-7>.
- [23] D. Xu, W. Wu, R. Malhotra, J. Chen, B. Lu, and J. Cao, “Mechanism Investigation for the Influence of Tool Rotation and Laser Surface Texturing (LST) on Formability in Single Point Incremental Forming”, *International Journal of Machine Tools and Manufacture*, Vol. 73, Pp. 37–46, 2013. <http://dx.doi.org/10.1016/j.ijmactools.2013.06.007>.
- [24] G. Buffa, D. Campanella, and L. Fratini, “On the Improvement of Material Formability in SPIF Operation Through Tool Stirring Action”, *International Journal of Advanced Manufacturing Technology*, Vol. 66, Pp. 9–12, Pp. 1343–1351, 2013. <http://dx.doi.org/10.1007/s00170-012-4412-9>.
- [25] N.S. Namer, S.A. Nama, and M.T. Mazhir, “Influence of lubricant viscosity on the surface roughness of PEHD and PVC plastic sheets in single point incremental forming process”, *International Journal of Engineering and Applied Sciences*, Vol. 7, No. 2, Pp. 27-30, 2015.
- [26] N.S.M. Namer, S.A. Nama, and M.T. Mezher, “The influence of Nano particles additive on tribological properties of AA2024-T4 coated with TiN or SiN thin films”, *Journal of Mechanical Engineering Research and Developments (JMERD)*, doi: <http://doi.org/10.26480/jmerd.03.2019.30.34>.
- [27] ASTM E8M-04 standard, Standard test methods for tension testing of metallic materials. 2004.